Article

Glycyrrhizinic Acid and Phosphatidylcholine Combination as a Preventive Therapy for Experimental Murine Non-Alcoholic Steatohepatitis

Veronika A. Prikhodko [1,2,*], Tatyana M. Matuzok [1,2], Vadim E. Karev [3], Anna V. Karavaeva [4], Olga M. Spasenkova [5], Nadezhda V. Kirillova [5], Dmitry Yu. Ivkin [4] and Sergey V. Okovityi [1,2]

1   Department of Pharmacology and Clinical Pharmacology, Saint Petersburg State Chemical and Pharmaceutical University, 197376 Saint Petersburg, Russia; matuzok.tatyana@pharminnotech.com (T.M.M.); sergey.okovity@pharminnotech.com (S.V.O.)
2   Laboratory of Targeted Intra-Brain Drug Delivery, N.P. Bechtereva Institute of the Human Brain of the Russian Academy of Sciences, 197376 Saint Petersburg, Russia
3   Pediatric Research and Clinical Center for Infectious Diseases of the Federal Medical Biological Agency, 197022 Saint Petersburg, Russia; vadimkarev@yandex.ru
4   Centre for Experimental Pharmacology, Saint Petersburg State Chemical and Pharmaceutical University, 197376 Saint Petersburg, Russia; anna.karavaeva@pharminnotech.com (A.V.K.); dmitry.ivkin@pharminnotech.com (D.Y.I.)
5   Department of Biochemistry, Saint Petersburg State Chemical and Pharmaceutical University, 197376 Saint Petersburg, Russia; olga.spasenkova@pharminnotech.com (O.M.S.); nadezhda.kirillova@pharminnotech.com (N.V.K.)
*   Correspondence: veronika.prihodko@pharminnotech.com

Abstract: Non-alcoholic metabolic-associated steatohepatitis (MASH) is a condition characterized by increasingly high prevalence and incidence, and also represents an important unmet medical need when it comes to effective pharmacotherapy. In this work, we aimed to explore the therapeutic possibilities of the synergistic combined use of glycyrrhizinic acid (GA) and phosphatidylcholine (PC) to prevent experimental MASH. Adult C57Bl/6 mice were used to model dietary/toxic MASH and treated orally by either GA (34.3 mg/kg/d) or a GA + PC combination (34.3 + 158.1 mg/kg/d) for 3 months. Animal locomotion, behaviour, short-term memory, physical performance, neuromuscular joint function, blood biochemistry, and oxidative stress marker levels were evaluated, followed by histological examination of the liver, skeletal muscle and sciatic nerve with tissue ammonia and lipid content determination. Real-time polymerase chain reaction was used to measure the relative expression of several pathogenetic transcript markers. GA and PC showed moderate additive synergism in their anti-inflammatory, antioxidant, hypoammonaemic, hypoglycaemic, and pro-cognitive activities. Differential effects of the agents were seen in regard to anxiety- and depression-like behaviour as well as gene expression. Our results indicate partial pharmacological synergism between GA and PC and validate further research of its potential clinical applications.

Keywords: glycyrrhizinic acid; phosphatidylcholine; essential phospholipids; non-alcoholic steatohepatitis; non-alcoholic steatotic liver disease; combination therapy

1. Introduction

Metabolic-associated steatotic liver disease (MASLD) is characterized by excessive hepatic lipid accumulation, defined by the presence of steatosis in >5% of hepatocytes, in the absence of significant alcohol consumption or other causes of liver injury [1]. A total of 12–14% of MASLD cases are classified as a more aggressive form known as metabolic-associated steatohepatitis (MASH), which can progress rapidly to liver fibrosis, cirrhosis, and hepatocellular carcinoma. MASLD and MASH affect up to 25% of the global adult population, and, considered together, are the leading cause of chronic liver disease worldwide [2]. Due to the high heterogeneity of the pathogenesis of metabolic liver disease, the

term 'metabolic [dysfunction]-associated steatotic liver disease' (MASLD) has recently been proposed as a broader, inclusive alternative to the previously accepted 'non-alcoholic fatty liver disease' 'NAFLD' [3].

Today, MASLD/MASH is considered an important risk factor for neurodegeneration and cerebrovascular disease, cognitive and memory impairment, and mood disorders such as depression and anxiety [4,5]. Besides central disorders, MASH may also be associated with peripheral nerve damage, which is possibly related to insulin resistance; dyslipidaemia and lipotoxicity; sarcopenia and myosteatosis; chronic low-grade systemic inflammation; and endothelial dysfunction [6,7].

Glycyrrhizinic acid (GA), a pentacyclic triterpenoid saponin obtained from the root and rhizome extracts of liquorice *Glycyrrhiza glabra* L., demonstrates a wide spectrum of biological activity in vitro and in vivo, including hepatoprotective, anti-inflammatory [8], anti-ischemic, antioxidant, neuroprotective [9,10], and pro-cognitive [11] characteristics, as well as several other effects. The major mechanisms of action of GA most relevant to liver pathology and its associated complications appear to include the following:

- Inhibition of nuclear factor-κB (NF-κB) translocation to the cell nucleus and the subsequent pro-inflammatory shift in gene expression [12];
- Suppression of release of interleukins (IL) 6 and 10, (TNFα), and other pro-inflammatory cytokines downstream of NF-κB [12];
- Inhibition of CD4+ T-cell proliferation via the c-Jun N-terminal kinase (JNK)/mitogen-activated protein kinase (MAPK) and phosphoinositide 3-kinase (PI3K)/protein kinase B (PKB/AKT) pathways [12];
- Upregulation of the nuclear factor erythroid 2-related factor 2 (Nrf2) signalling and its downstream effectors, including antioxidant enzymes and anti-inflammatory messengers [13];
- Upregulation of nuclear peroxisome proliferator-activated receptor γ (PPARγ) [14];
- Modulation of the sirtuin deacetylase expression and activity [15], and other effects;

Via the above mechanisms, GA is able to invoke a potent systemic and local anti-inflammatory response, suppress hepatocyte apoptosis and necrosis, reduce hepatic and systemic insulin resistance, normalize glucose and lipid homoeostasis, and promote liver regeneration [16].

Phosphatidylcholine ((3-sn-phosphatidyl)choline, PC), the major constituent of essential phospholipid preparations, is the most abundant phospholipid within the cell membrane. Besides replacing the damaged and oxidized membrane lipids [17], PC is hypothesized to act as a direct endogenous ligand for PPARα, or activate them via sirtuin upregulation, stimulating fatty acid β-oxidation in hepatocytes. PC may also alter the activity of sterol regulatory-element-binding proteins (SREBP) and SREBP-dependent enzymes, which leads to the inhibition of de novo lipogenesis, fatty acid uptake, and cholesterol biosynthesis. Finally, PC may promote lipoprotein-mediated fatty acid evacuation from the liver followed by their uptake and utilization in skeletal muscle [18].

Besides direct hepatoprotection on its own, PC may form nanoliposomes and act as a carrier system for GA, thus improving its oral bioavailability and further increasing its pharmacological effects [19]. In view of the above, this study was performed to assess the effects of a glycyrrhizinic acid + phosphatidylcholine combination as a preventive therapy regimen for hepatic dysfunction and associated disorders in experimental murine MASH.

2. Materials and Methods

The animal study protocol was written in full compliance with the principles of the Basel Declaration, the European Convention for the Protection of Vertebrate Animals used for Experimental and other Scientific Purposes (European Treaty Service No. 123, 18 March 1986), and the Order of the Ministry of Health of the Russian Federation No. 199n (1 April 2016) "On the approval of the Rules of Good Laboratory Practice", and was approved by the Bioethics Committee of the St. Petersburg State Chemical and Pharmaceutical University,

as governed by the Ministry of Health of the Russian Federation (protocol M-GAPC-PS-22; 10 January 2022).

A total of 100 young-adult (2 month old) male C57Bl/6J mice weighing 18–20 g were purchased from the Stolbovaya laboratory animal supplier (Moscow Oblast, Russia). All animals were received in a single shipment, quarantined for 2 weeks, then housed in a standard animal facility with ad libitum access to standard chow and drinking water. Prior to experimentation, the animals were randomized into 4 groups:

1. Intact ($n = 10$), standard diet + 0.1 mL almond oil intraperitoneally (i/p) once weekly (q.wk.);
2. Control ($n = 30$), high-fat diet (HFD) + 0.32 mg/kg CCl_4 i/p q.wk;
3. Glycyrrhizinic acid (GA) ($n = 30$), HFD + 34.3 mg/kg/d GA p/o + 0.32 mg/kg CCl_4 i/p q.wk;
4. Glycyrrhizinic acid + phosphatidylcholine (GAPC) ($n = 30$), HFD + 34.3 mg/kg/d GA p/o + 158.1 mg/kg PC p/o + 0.32 mg/kg CCl_4 i/p q.wk.

MASH was induced over 3 months using the model described by Tsuchida et al. [20], combining a "western"-like HFD and low-dose i/p CCl_4 as an accelerant. GA and PC were incorporated into the HFD pellets at calculated weight concentrations in order to allow for the required daily intake for each mouse. The pellets were prepared ex tempore in our laboratory and contained 50.9% standard chow (compound feed LBK-120; Tosnensky Mixed Feed Factory, Nurma, Russia), 16.1% beef tallow, and 33.0% D-fructose. These proportions were calculated with regard to the chow fat and fibre content so that the resulting composition would yield 21.1% total fat and 41% total carbohydrates and match the diet described by Tsuchida et al. [20]. For the GA group, the remaining standard chow content was slightly lowered in order to include the additional 0.02% GA (trisodium glycyrrhizinate; Pharmstandard, Kursk, Russia) (equivalent to a 195 mg/d human dose or a 34.3 mg/kg/d mouse dose calculated using the conversion coefficient recommended by the Food and Drug Administration [21]). For the GAPC group, an additional adjustment was made in order to include 0.11% PC (Lipoid PPL-400 containing 73–79 PC; Pharmstandard, Kursk, Russia) (equivalent to a 900 mg/d human dose or a 158.1 mg/kg/d mouse dose calculated using the same coefficient). The human GA and PC doses were chosen according to the manufacturer's (Phosphogliv forte, Pharmstandard, Kursk, Russia) dosage recommendations [22].

Animal locomotor activity and behaviour were assessed using the open field (OF), elevated plus maze (EPM), and light/dark box (LDB) tests (Open Science, Krasnogorsk, Russia). Animal movement was recorded on camera for 3 min and analysed subsequently using the VideoMot2 3.0.1 (TSE Systems GmbH, Bad Homburg, Germany) (for OF and LDB) or RealTimer 1.30 (Open Science, Krasnogorsk, Russia) (for EPM) software.

In the OF test, distance covered (cm), mean velocity ($cm \cdot s^{-1}$), time in centre (s), total freezing duration (s), and the number of freezes, line crossings, rears, grooming bouts, and hole pokes were registered [23]. In the EPM test, time spent in the open arms, closed arms, and centre (s), the number of entries into the open and closed arms, rears, grooming bouts, head dips, and peeking-out frequency were registered [24]. In the LDB test, time spent (s) and distance covered (cm) in the white chamber (WC); mean velocity ($cm \cdot s^{-1}$); total freezing duration (s); instances of freezing, grooming, and rearing (min^{-1} in the WC); as well as peeking-out frequency (min^{-1} in the dark chamber (DC)); the number of transitions; latency in entering the DC for the 1st time (s); and duration of the 1st DC visit (s) were registered [25].

Depression-like behaviour was assessed using the tail suspension (TS), forced swim (FS), and sucrose splash (SS) tests. In the TS [26] and FS [27] tests, the number of immobility episodes, total duration of immobility (s), and latency to the 1st immobility episode (s) were registered using the RealTimer software. In the SS test, total distance travelled (cm), the number of grooming bouts, and total grooming duration (s) were registered [28].

Short-term spatial memory and object-recognition memory were assessed using the spontaneous alternation in the T-maze (SATM) and novel-object recognition (NOR) tests,

respectively. In the SATM test, spontaneous alternation percentage was assessed live by an experienced researcher, in 3 trials per animal [29]. In the NOR test, total object exploration time (s) and novel-object exploration time (s) were registered using the RealTimer software, and the discrimination index was calculated as described previously [30].

Blood ammonia (µmol/L) and lactate (mmol/L) levels were assessed by reflectance photometry in whole-blood samples obtained from the tail vein using the PocketChem BA PA-4140 (Arkray, Japan) and Accutrend Plus (Roche, Germany) systems, respectively. Serum alanine aminotransferase (ALT; international unit (IU)/L), aspartate aminotransferase (AST; IU/L), alkaline phosphatase (ALP; IU/L), total protein (g/L), cholesterol (mmol/L), and glucose (mmol/L) levels were measured using the Erba XL-100 biochemical analysis system (Mannheim, Germany) with compatible Erba SysPack reagents.

Animal physical performance was assessed using the three-trial 7.5% b.w. weight-loaded exhaustive swim test (TTES). Swimming time was registered at the start (1st trial), 5 min after the completion of the 1st trial (2nd trial), and 45 min after the completion of the 2nd trial (3rd trial) [31].

An electroneuromyographical (ENMG) study was conducted using the 8-channel Neuro-MEP-8 ENMG system with Neuro-MEP.NETω 3.7.3.7 software (Neurosoft, Ivanovo, Russia). Before the procedure, the animals were anaesthetized with chloral hydrate (Milli-poreSigma, Burlington, MA, USA; 400 mg/kg i/p). Compound muscle action potentials (CMAP) were registered in the left m. gastrocnemius under left n. ischiadicus (pl. lumbalis) stimulation and in the right m. biceps brachii under right n. musculocutaneus (pl. brachialis) stimulation [32]. For electrical stimulation, rectangle-shaped 0.1 ms stimuli were used, with currents going from 1 to 10 mA in increments of 1 mA in order to achieve supramaximal stimulation. The signal input range was 500 mV, the frequency filter, 5 Hz–10 kHz, and the sample rate, 20 kHz.

Following the completion of all experiments, the mice were euthanized by carbon dioxide inhalation, and the liver, m. gastrocnemius, n. ischiadicus, heart, kidney, and brain were excised for histological examination. Tissue samples were fixed in 10% buffered formalin, dehydrated, cleared in isopropanol, and embedded in paraffin according to standard protocols. Subsequently, 4 µm sections prepared from paraffin blocks were mounted on slides, stained with haematoxylin and eosin or Van Gieson's picrofuchsin, cover-slipped, and examined using light microscopy. For each tissue sample, each kind of pathological change was scored as 0 (no), 1 (mild), 2 (moderate), or 3 (severe).

Ammonia levels were assessed in the liver, heart, kidney, brain, n. ischiadicus and skeletal muscle using Nessler's reagent according to a previously published protocol [33]. Liver and muscle steatosis was assessed using Sudan III, also according to a conventional protocol. Tissue lipid and ammonia contents were graded using the system described above.

Serum malondialdehyde (MDA) concentration (nmol/mL) was measured using a spectrophotometric assay of its complex with thiobarbituric acid, as described by N.A. Botsoglou et al. [34] Serum catalase activity (µmol/mg/min) was measured using a spectrophotometric assay of hydrogen peroxide based on formation of its stable complex with ammonium molybdate, as described by L. Góth [35]. Serum superoxide dismutase (SOD) activity (% inhibition) was measured using an indirect method, based on inhibition of quercetin autooxidation, as described by V.A. Kostiuk et al. [36] Erythrocyte carbonyl content was determined using a slight modification of the method described by R.L. Levine et al. [37], which is based on the spectrophotometric assay of aldo- and ketohydrazones formed by oxidized amino acids with 2,4-dinitrophenylhydrazine.

Total RNA was extracted from homogenized tissues by using the ExtractRNA® agent (Evrogen, Moscow, Russia), and cDNA was synthesised using a MMLV RT® kit (Evrogen, Moscow, Russia). RT-qPCR was performed in a CFX96 Touch RT-PCR system (Bio-Rad, Hercules, CA, USA) using a 5X qPCRmix-HS SYBR® kit (Evrogen, Moscow, Russia) under the following thermal cycling conditions: 5 min at 95 °C, followed by 40 cycles composed of 10 s at 95 °C, 15 s at 63 °C, and 15 s at 72 °C. The relative expression of Apoa1 (apolipoprotein 1, ApoA1), Il1b (interleukin 1β, IL1β), Scd1 (stearoyl-coenzyme A desaturase, SCD1), Des

(desmin), and Col4 (collagen IV) in the liver, as well as Fndc5 (fibronectin type III domain-containing protein 5, FNDC5), Mstn (myostatin), and Myog (myogenin) in skeletal muscle, was quantified using the ΔΔCt method. Actb (β-actin) was used as a housekeeping gene. All samples were run in triplicates. The primers were obtained from Evrogen (Moscow, Russia); primer sequences are given in Table 1.

Table 1. Primer sequences.

Gene	Forward Primer, 5′-3′	Reverse Primer, 5′-3′
Apoa1	GTGGCTCTGGTCTTCCTGAC	ACGGTTGAACCCAGAGTGTC
Il1b	CTGCAGCTGGAGAGTGTGGAT	CTCCACTTTGCTCTTGACTTCTATCTT
Scd1	CCGGAGACCCCTTAGATCG	TAGCCTGTAAAAGATTTCTGCAAACC
Des	AAGATGGCCTTGGATGTGGA	GTTGATCCTGCTCTCCTCGC
Col4	TGATAAAGGTTCCCGAGGAG	ATCCTGGTGTCCCACTAAGG
Fndc5	ACAGGCAGAGAGCAGAGAGC	GAAGTCTGCTGCCACATCAA
Mstn	AGTGGATCTAAATGAGGGCAGT	GTTTCCAGGCGCAGCTTAC
Myog	GGGCAATGCACTGGAGTT	CACGATGGACGTAAGGGAGT
Actb	AAGATCCTGACCGAGCGTGGCT	AGGGAGGAAGAGGATGCGGCAG

Statistical analysis was carried out in Prism 9.0.0 (GraphPad Software, San Diego, CA, USA) and R 4.3.0 (R Foundation for Statistical Computing, Indianapolis, IN, USA) with RStudio 2023.06.0+421 (RStudio PBC, Boston, MA, USA). Data were tested for normality using the Shapiro–Wilk test, then tested for significant differences using one-way ANOVA followed by Dunnett's post hoc test (for normally distributed data), or the Kruskal–Wallis non-parametric test followed by Dunn's post hoc test (if otherwise). Semiquantitative analysis of scored histology data was conducted using the RVAideMemoire 0.9-81-2 function package for R [38], as described previously [39]. Mortality was assessed using the Kaplan–Meier method, and the survival curves were compared using the log-rank (Mantel-Cox) test; hazard ratios were calculated using the Mantel–Haenszel method. Data are presented as mean ± standard-error-of-mean in the bar plots, and as minimum, lower quartile, mean, upper quartile, and maximum in the box-and-whisker plots. The significance threshold was set at $p < 0.05$.

3. Results

3.1. Tissue Morphology

3.1.1. Liver

Most liver samples from the Intact group showed signs of mild hepatitis (METAVIR-A 1), mild or moderate granulomatous hepatitis, no (or mild) steatosis, and the occasional presence of small necrotic foci. None of the samples had hepatocellular ballooning or cholestasis, and, despite a few samples having few fibrous septae, all were graded as 0 (no fibrosis) according to the METAVIR-F scale (Figures 1 and 2).

Control samples demonstrated predominantly moderate-to-severe hepatitis (METAVIR-A 2/3), moderate granulomatous hepatitis, mild-to-moderate macro- and microvesicular steatosis, hepatocellular ballooning of varying severity, mild cholestasis, extensive tissue necrosis, and septal fibrosis. Significant ($p < 0.05$ for all) differences from the Intact group were registered for steatosis, cholestasis, and the presence of fibrous septae (Figure 1). Morphological score totals were significantly ($p < 0.05$) higher in the Control group compared to the Intact group.

No significant differences were found between the Control and GA groups. The GAPC treatment regimen improved the severity of granulomatous hepatitis ($p < 0.05$), but had no significant effect on other liver morphology parameters (Figure 2).

3.1.2. Skeletal Muscle

In all experimental groups, mild-to-moderate skeletal muscle fibre dystrophy, cell exudation, reactive perimysium proliferation, and mild interstitial fibrosis were observed;

several samples showed signs of partial compensatory hypertrophy of muscle fibres. All pathological changes tended to be more pronounced in the Control group; however, this tendency was non-significant (Figures 3 and 4).
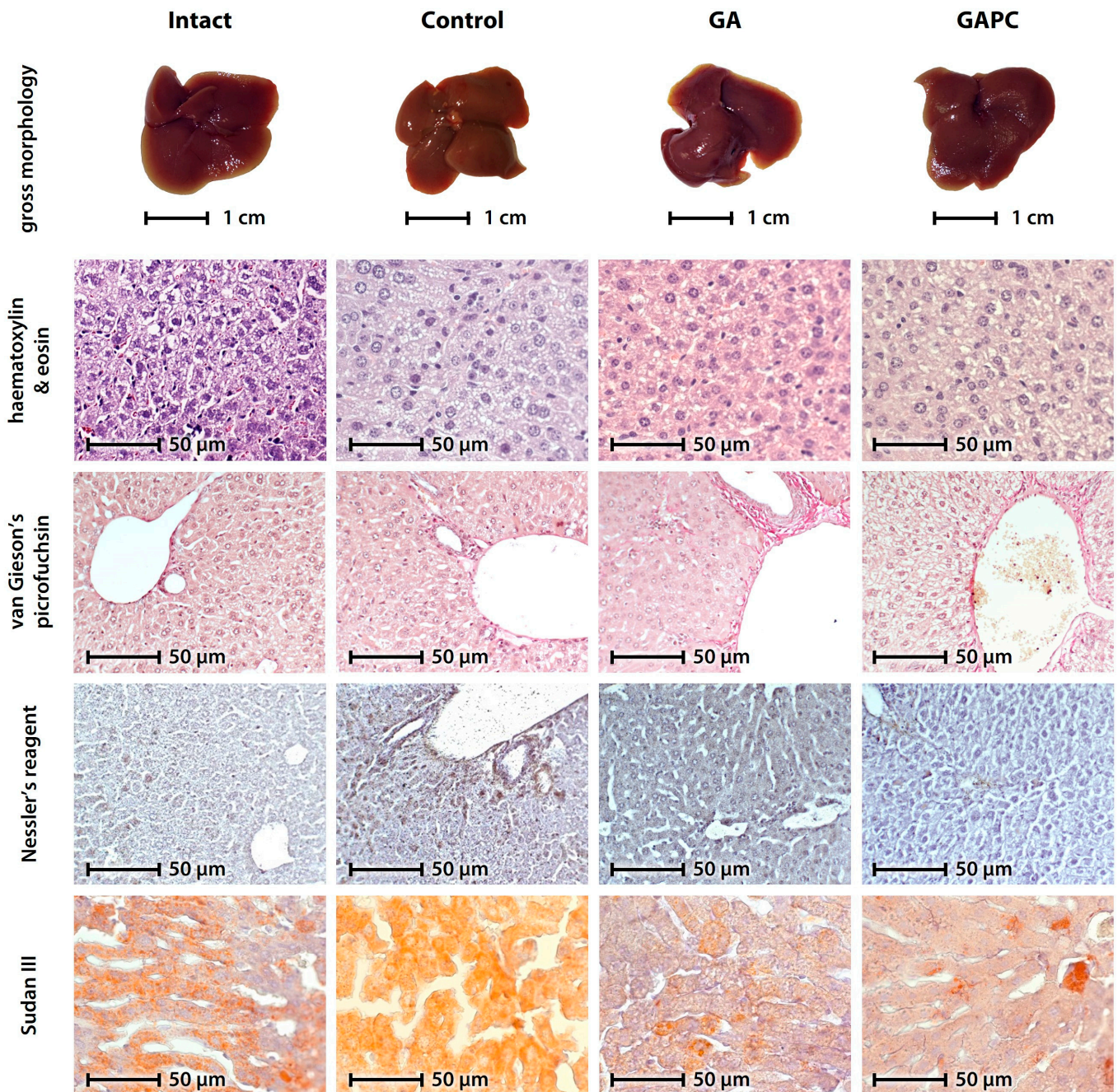

Figure 1. Liver morphology. All slides: ×200. GA, Glycyrrhizinic acid; GAPC, Glycyrrhizinic acid + phosphatidylcholine.
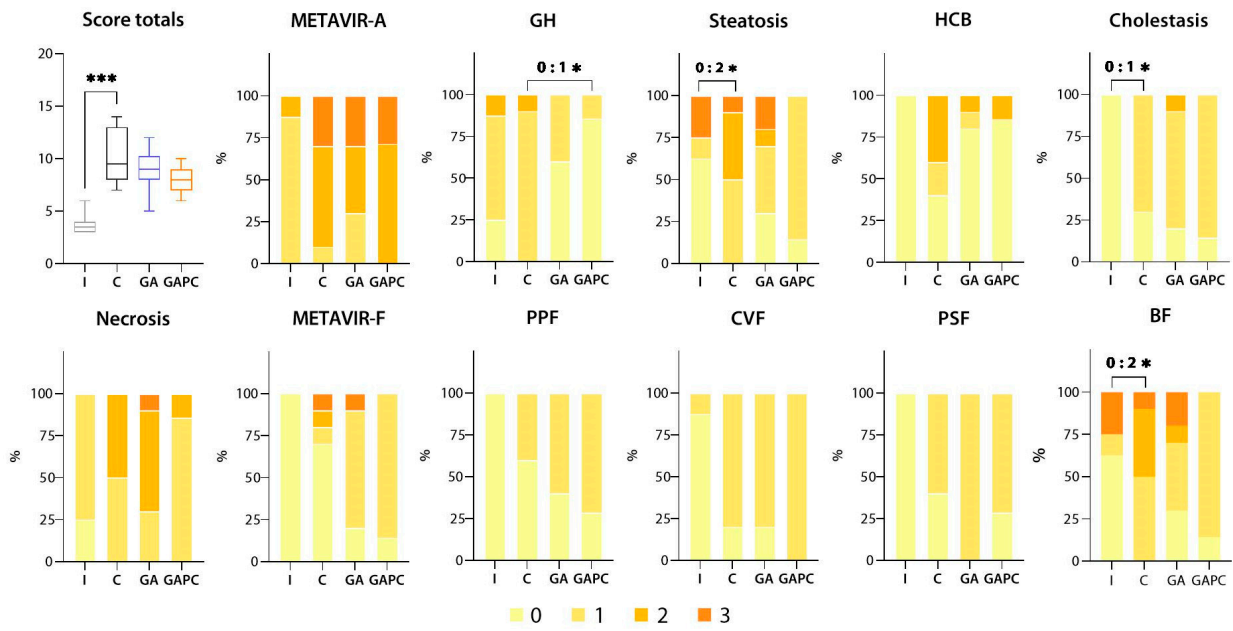
Figure 2. Morphological score frequency contingencies for the liver. I, Intact; C, Control; GA, Glycyrrhizinic acid; GAPC, Glycyrrhizinic acid + phosphatidylcholine; GH, granulomatous hepatitis; HCB, hepatocellular ballooning; PPF, periportal fibrosis; CVF, central vein fibrosis; PSF, perisinusoidal fibrosis; BF, bridging fibrosis; * $p < 0.05$; *** $p < 0.001$.
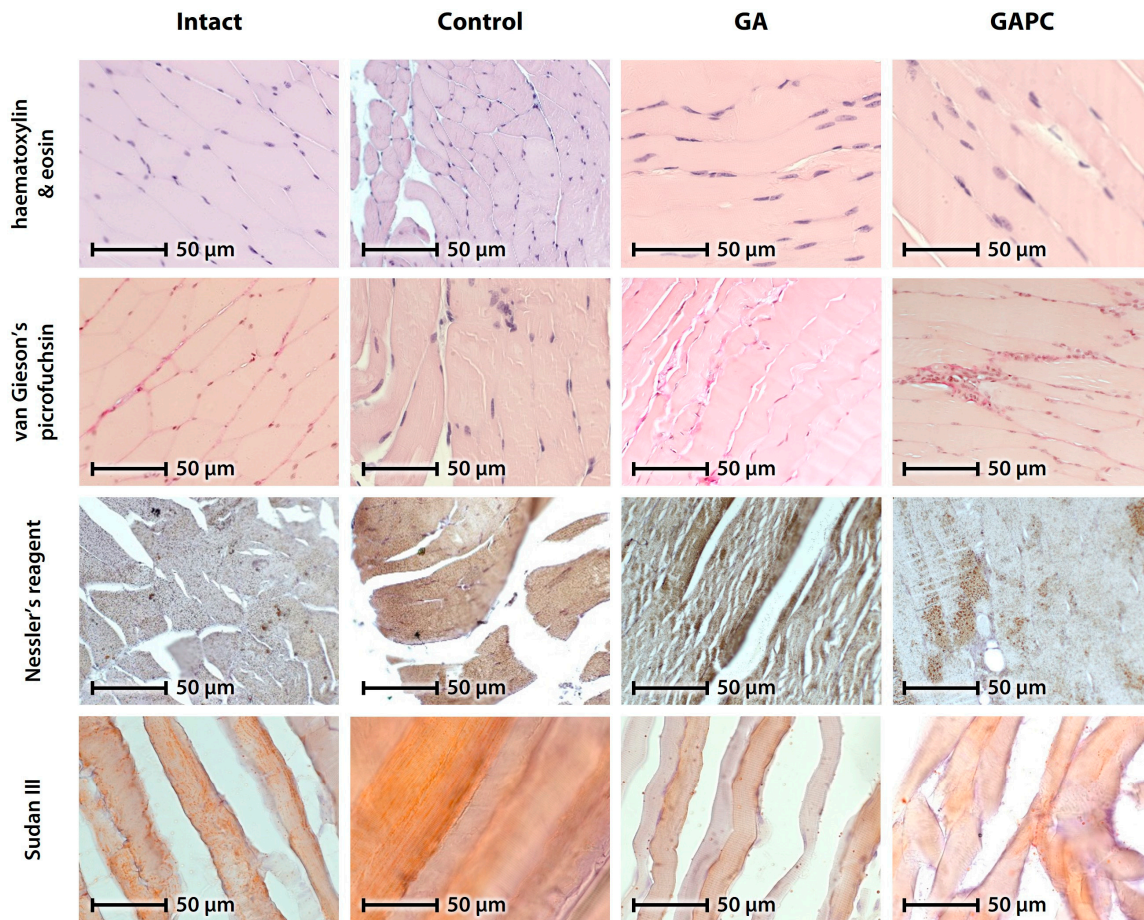

Figure 3. Skeletal muscle morphology. All slides: ×200. GA, Glycyrrhizinic acid; GAPC, Glycyrrhizinic acid + phosphatidylcholine.
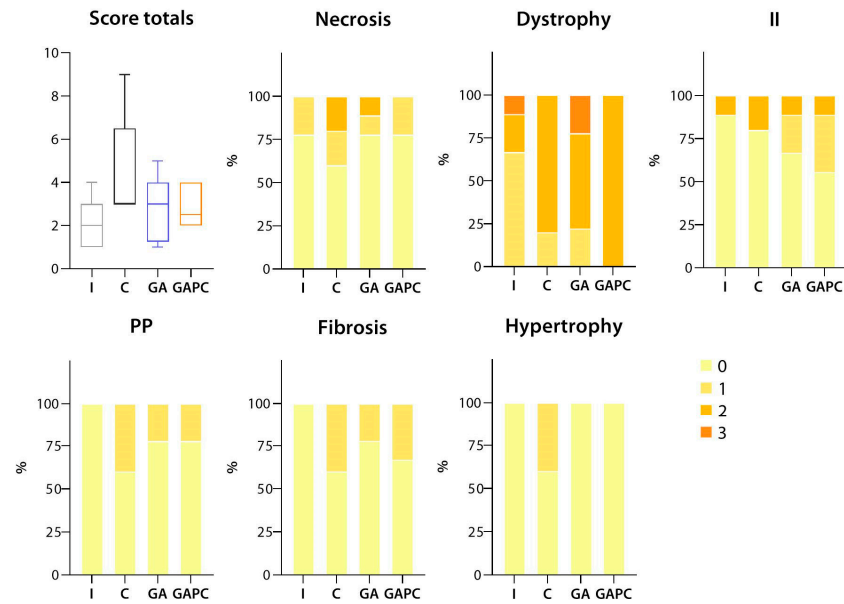
Figure 4. Morphological score frequency contingencies for the skeletal muscle. I, Intact; C, Control; GA, Glycyrrhizinic acid; GAPC, Glycyrrhizinic acid + phosphatidylcholine; II, interstitial infiltrate; PP, perimysium proliferation.

3.1.3. Sciatic Nerve

In most samples obtained from mice from the Intact group, moderate nerve fibre vacuolization with mild or moderate intercellular oedema was observed; several samples exhibited additional signs of degeneration and fibre fragmentation. In the Control group, fibre vacuolization was accompanied by moderate intercellular oedema, with a few samples showing signs of basophilic degeneration. Mice that had been receiving GA showed signs of moderate nerve fibre vacuolization and basophilic degeneration, accompanied by (mostly moderate) intercellular oedema. In the GAPC group, moderate fibre vacuolization and oedema were generally not associated with degenerative changes (Figures 5 and 6).
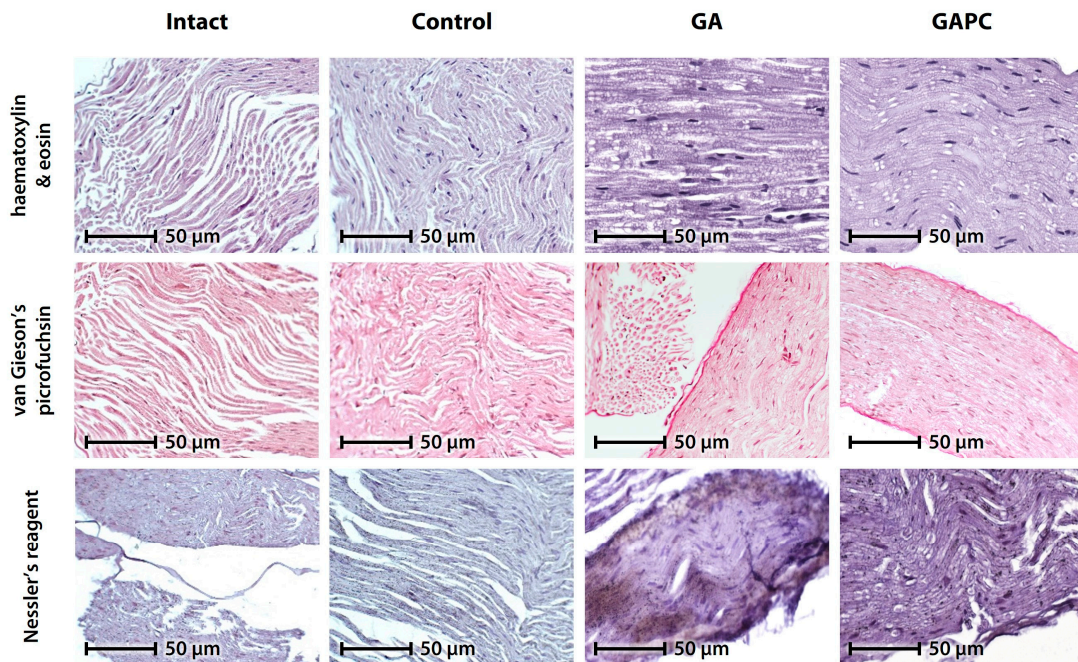

Figure 5. Sciatic nerve morphology. All slides: ×200. GA, Glycyrrhizinic acid; GAPC, Glycyrrhizinic acid + phosphatidylcholine.
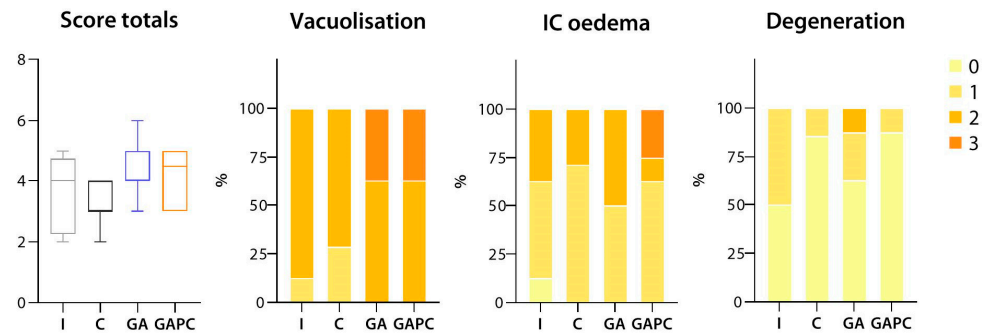
Figure 6. Morphological score frequency contingencies for the sciatic nerve. I, Intact; C, Control; GA, Glycyrrhizinic acid; GAPC, Glycyrrhizinic acid + phosphatidylcholine; IC, intercellular.

3.1.4. Tissue Lipid Content

Steatosis was significantly ($p < 0.05$) more pronounced in Control group liver and muscle samples than in Intact ones. Both GA and GAPC reduced tissue lipid content to normal levels ($p < 0.01$ vs. Control for GA, $p < 0.05$ vs. Control for GAPC). Despite the apparent non-significance of the differences due to the limitations of our analysis method, there was a clear tendency towards an increase in liver microvesicular steatosis and myosteatosis; both were effectively countered by the experimental treatment regimens (Figure 7).
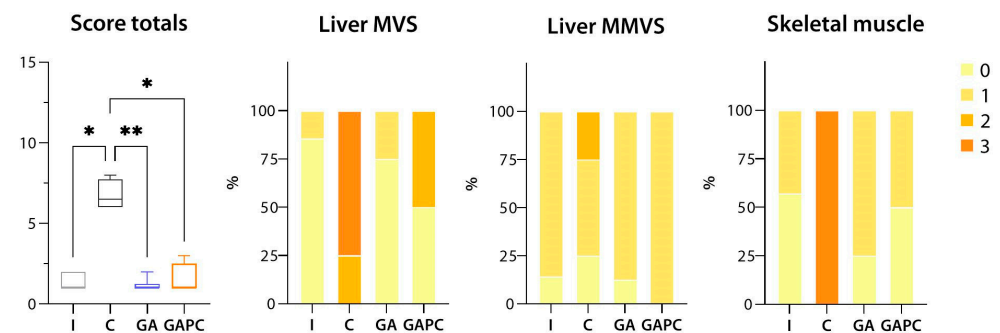

Figure 7. Score frequency contingencies for tissue lipid content. I, Intact; C, Control; GA, Glycyrrhizinic acid; GAPC, Glycyrrhizinic acid + phosphatidylcholine; MVS, microvesicular steatosis; MMVS, medio- and macrovesicular steatosis; * $p < 0.05$; ** $p < 0.01$.

3.1.5. Tissue Ammonia Content

Ammonia accumulation was significantly ($p < 0.01$) greater in the tissues of mice from the Control group compared to the Intact mice. It was reduced to Intact levels by both treatment regimens; however, this change only proved statistically significant in the GA group ($p < 0.05$ vs. Control). Ammonia deposition by organ did not differ significantly among the groups, albeit a slight tendency towards increased ammonia levels was observed for Control skeletal muscle, heart, and kidney samples (Figure 8).

3.2. Blood Biochemistry

In the Control group, we observed a significant increase in serum glucose and blood ammonia levels ($p < 0.05$, $p < 0.0001$, respectively). Serum AST, ALT, ALP, total protein, cholesterol, triglycerides, and blood lactate levels remained unchanged. GA treatment reduced blood ammonia levels ($p < 0.05$ vs. Control), and GAPC reduced both serum glucose and blood ammonia concentrations ($p < 0.05$, $p < 0.01$ vs. Control, respectively) (Figure 9).
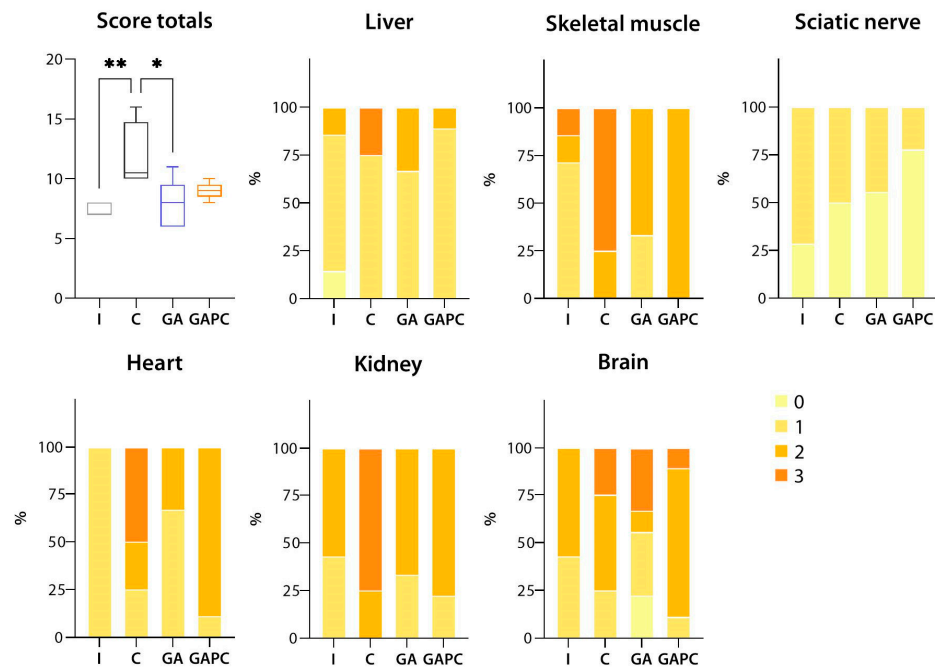
Figure 8. Score frequency contingencies for tissue ammonia content. I, Intact; C, Control; GA, Glycyrrhizinic acid; GAPC, Glycyrrhizinic acid + phosphatidylcholine; * $p < 0.05$; ** $p < 0.01$.
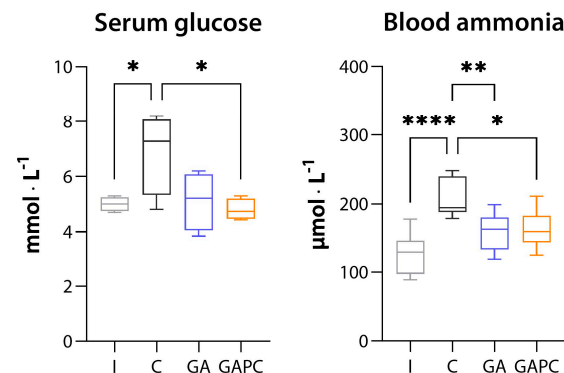

Figure 9. Blood biochemistry parameters. I, Intact ($n = 10$); C, Control ($n = 6$); GA, Glycyrrhizinic acid ($n = 10$); GAPC, Glycyrrhizinic acid + phosphatidylcholine ($n = 10$); * $p < 0.05$; ** $p < 0.01$, ****, $p < 0.0001$.

3.3. Oxidative Stress

MDA levels were doubled in the Control group compared to Intact mice ($p < 0.01$); both GA and GAPC reduced them by approximately 30% ($p < 0.01$ for both). Catalase activity was reduced in the Control group ($p < 0.05$ vs. Intact) and rescued to Intact levels in the GAPC ($p < 0.05$ vs. Control), but not in the GA group. SOD activity was without significant change among the groups. Erythrocyte neutral carbonyl content was significantly ($p < 0.01$ vs. Intact) increased in the Control group and reduced to normal levels in both treatment groups ($p < 0.01$ vs. Control for both). The increase in Erythrocyte basic carbonyl content in Control mice failed to reach statistical significance; however, in the GA group, it was significantly ($p < 0.05$) lower than in the Control group (Figure 10).
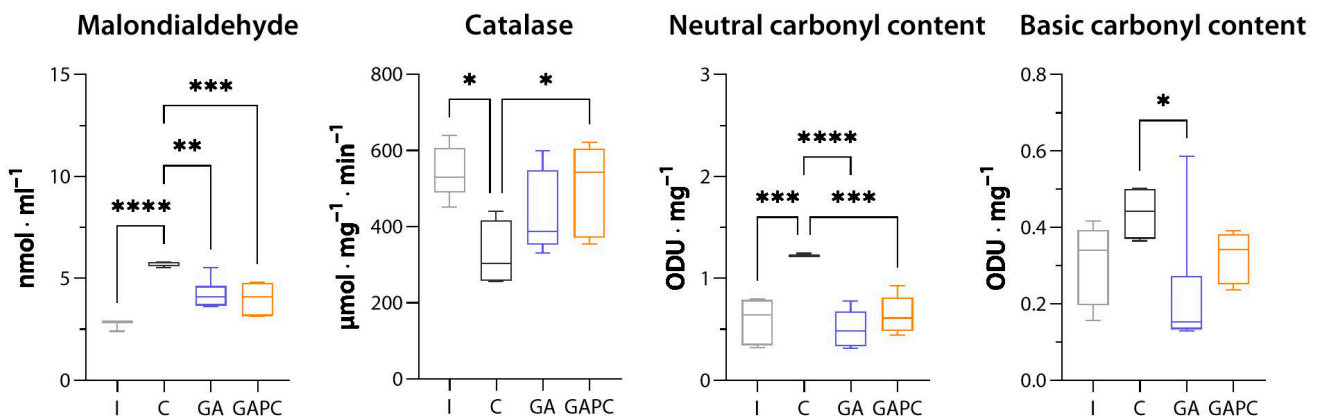
Figure 10. Oxidative stress marker levels. I, Intact (*n* = 10); C, Control (*n* = 6); GA, Glycyrrhizinic acid (*n* = 10); GAPC, Glycyrrhizinic acid + phosphatidylcholine (*n* = 10); ODU, optical density unit; * $p < 0.05$; ** $p < 0.01$; *** $p < 0.001$; **** $p < 0.0001$.

3.4. RT-qPCR

RT-qPCR showed that Apoa1 relative mRNA expression was increased in the GA group ($p < 0.01$ vs. Control), and Des expression was increased in the Control group ($p < 0.01$ vs. Intact). Moreover, Fndc5 transcript expression was increased markedly, although to a statistically insignificant degree, in the Control group, and reduced in both the GA and GAPC groups. Il1b, Scd1, Col4, Mstn and Myog expression levels were all without notable change (Figure 11).

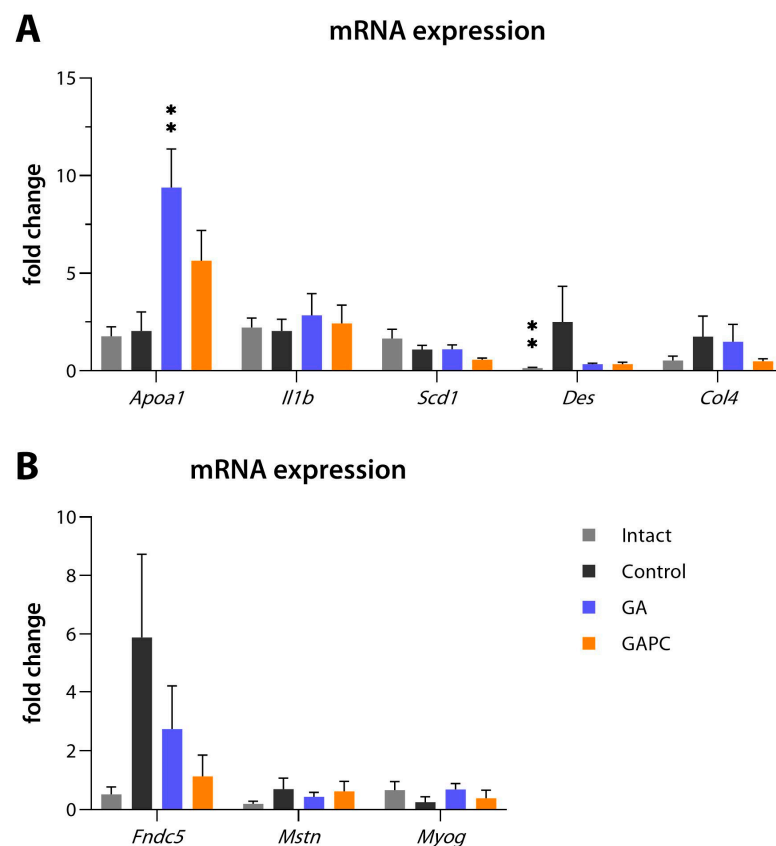**Figure 11.** Relative mRNA expression in liver (**A**) and skeletal muscle (**B**) tissue. Intact (*n* = 10); Control (*n* = 6); GA, Glycyrrhizinic acid (*n* = 10); GAPC, Glycyrrhizinic acid + phosphatidylcholine (*n* = 10); ** $p < 0.01$ vs. Control.

3.5. Locomotion, Behaviour, and Memory

3.5.1. General Locomotion and Anxiety-like Behaviour

In the OF test, Control mice had significantly ($p < 0.01$ for both) reduced mean velocity and hole poking frequency, while in the EPM test, they demonstrated markedly reduced peeking-out frequency ($p < 0.01$). There was a slight tendency towards an increase in all listed parameters in the GA and GAPC groups, but it failed to reach statistical significance (Figure 12A,B).
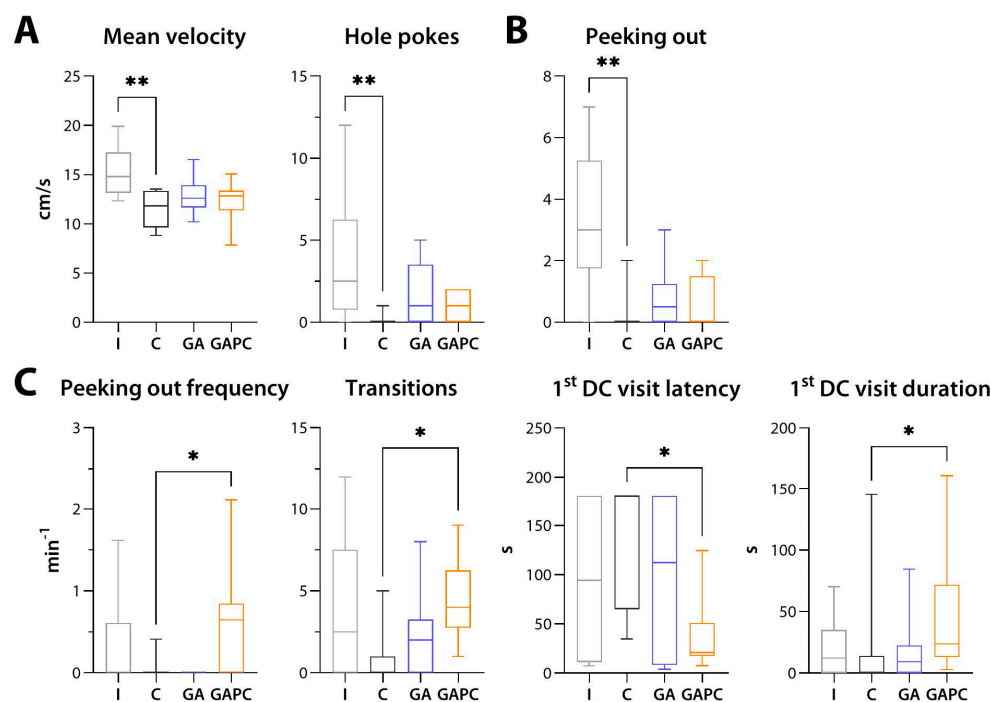

Figure 12. (**A**) General locomotion and exploratory activity, as assessed by the open field test. (**B**) Anxiety-like behaviour as assessed by the elevated plus maze test. (**C**) Anxiety-like behaviour as assessed by the light/dark box test. I, Intact ($n = 10$); C, Control ($n = 6$); GA, Glycyrrhizinic acid ($n = 10$); GAPC, Glycyrrhizinic acid + phosphatidylcholine ($n = 10$); DC, dark chamber; * $p < 0.05$; ** $p < 0.01$.

In the LDB test, no apparent changes were detected between the Intact and Control groups. GAPC, but not GA alone, increased the peeking-out frequency and the number of chamber transitions, as well as latency to the first visit to the dark chamber, and its duration ($p < 0.05$ for all). For peeking-out frequency, the effect of GAPC was significantly superior to that of GA monotherapy ($p < 0.01$) (Figure 12C).

3.5.2. Depression-like Behaviour

In the TS test, GAPC treatment increased the latency to the first immobility episode ($p < 0.05$ vs. Control), and in the SS test, it increased total duration of grooming compared to GA monotherapy ($p < 0.05$) but not Control. In the FS test, immobility episode frequency ($p < 0.01$) and duration ($p < 0.05$) were greatly reduced in mice that had been receiving GA, and immobility latency was increased in both treatment groups compared to Control ($p < 0.01$ for GA, $p < 0.05$ for GAPC) (Figure 13).
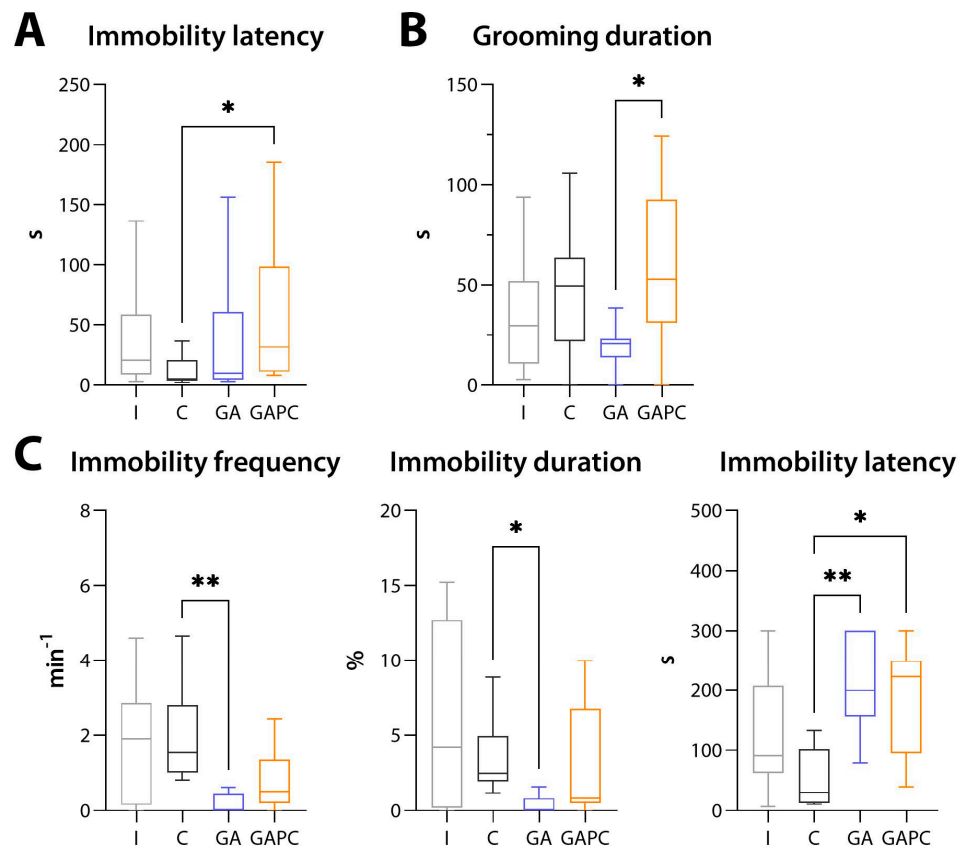
Figure 13. Depression-like behaviour as assessed by the (**A**) tail suspension test, (**B**) sucrose splash test, and (**C**) forced swim test. I, Intact (*n* = 10); C, Control (*n* = 6); GA, Glycyrrhizinic acid (*n* = 10); GAPC, Glycyrrhizinic acid + phosphatidylcholine (*n* = 10); * *p* < 0.05; ** *p* < 0.01.

3.5.3. Memory

In the SATM test, Control group mice had a lower alternation rate than did Intact ones (*p* < 0.05). GA alone only partially improved it, while the GAPC combination restored it to Intact values (*p* < 0.05 vs. Control) (Figure 14A).

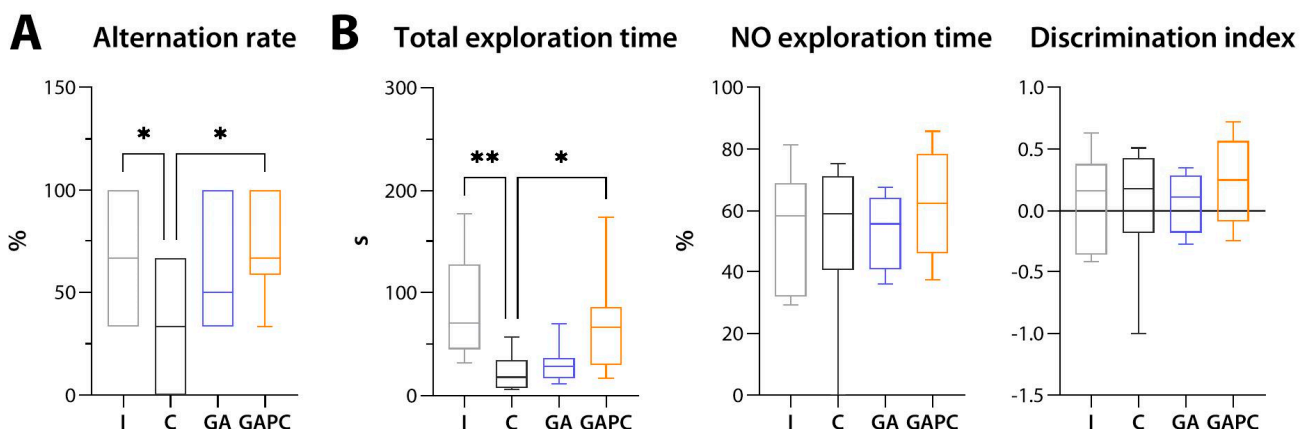**Figure 14.** (**A**) Short-term spatial memory as assessed by the spontaneous alternation in the T-maze test. (**B**) Short-term recognition memory as assessed by the novel-object recognition test. I, Intact (*n* = 10); C, Control (*n* = 6); GA, Glycyrrhizinic acid (*n* = 10); GAPC, Glycyrrhizinic acid + phosphatidylcholine (*n* = 10); NO, novel object; * *p* < 0.05; ** *p* < 0.01.

In the NOR test, total exploration was reduced in the Control group compared to the Intact group ($p < 0.01$). GAPC significantly improved it ($p < 0.05$ vs. Control), while GA alone had no notable effect. No differences in novel-object exploration time or discrimination index values were observed among the groups (Figure 14B).

3.6. Physical Performance

In the TTES test, swimming time was greatly reduced for Control mice in all trials ($p < 0.01$ vs. Intact). GA or GAPC treatment had no effect on either basal physical performance or recovery rates, as indicated by the unchanged trial index values (Figure 15).
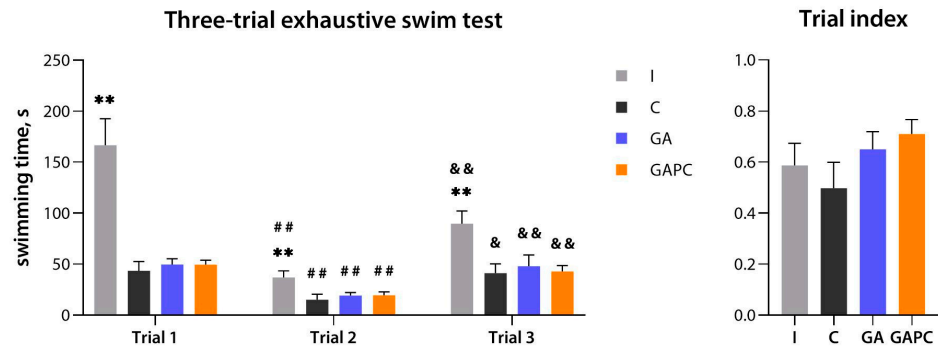

Figure 15. Physical performance as assessed by the three-trial exhaustive swim test. I, Intact; C, Control; GA, Glycyrrhizinic acid; GAPC, Glycyrrhizinic acid + phosphatidylcholine; ** $p < 0.01$ vs. Control; ## $p < 0.01$ vs. trial 1; & $p < 0.05$ vs. trial 2; && $p < 0.01$ vs. trial 2.

3.7. ENMG

The ENMG study detected no change in neuromuscular joint function parameters in Control mice, albeit a small (non-significant) reduction of CMAP peak amplitude was present. Both GA and GAPC treatment regimens improved peak amplitudes in both m. gastrocnemius and m. biceps brachii ($p < 0.01$ for GA for both, $p < 0.05$ for GAPC for both) (Figure 16).
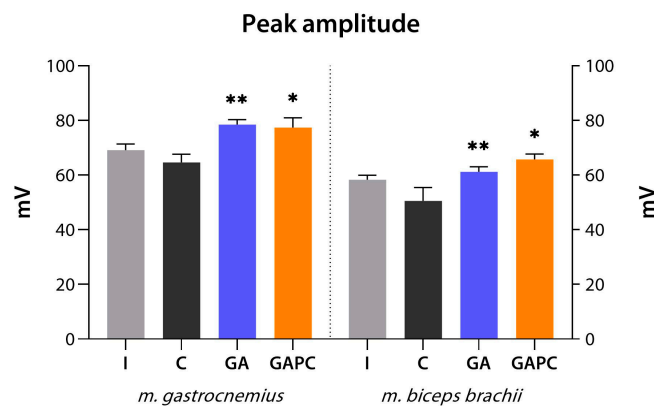

Figure 16. Compound muscle action potential parameters. I, Intact; C, Control; GA, Glycyrrhizinic acid; GAPC, Glycyrrhizinic acid + phosphatidylcholine; * $p < 0.05$; ** $p < 0.01$ vs. Control.

4. Discussion

MASH is morphologically characterized by the presence of liver steatosis, lobular inflammation, and hepatocyte ballooning, and is frequently accompanied by intrahepatic cholestasis and other histological abnormalities [40]. In our study, all the above features, as well as periportal, central vein, and perisinusoidal fibrosis, in addition to fibrous septa, were present with no signs of cirrhosis, which is indicative of the MASH/fibrosis stage of the disease.

Inflammation is the key process defining MASH, and is considered one of the primary pathogenetic targets for glycyrrhizinic acid preparations [12]. In our study, the GAPC combination, but not GA alone, reduced the activity of granulomatous hepatitis in mice. While the synergistic anti-inflammatory effects of GA and PC could possibly be the result of GA's bioavailability being enhanced by PC, they could also be explained by the fact that both agents are capable of alleviating the inflammatory response in the liver. PC has been shown to inhibit the differentiation of pro-inflammatory liver M1-type macrophages, most likely due to TLR-2-mediated metabolic reprogramming [41,42]. Some in vitro studies have also demonstrated that PC is able to regulate NF-κB activation [43,44], which could augment the effects of GA on this pathway [12].

Both GA and GAPC markedly improved total tissue lipid content, mainly alleviating liver microvesicular steatosis and myosteatosis. The two agents could exert synergistic effects on lipid metabolism via several shared mechanisms, namely, PPARα/γ upregulation [14,18,45] and downregulation of SREBP-1c and its downstream lipogenic enzymes [18,46].

GA reduced total tissue ammonia content, with the most pronounced effects on the skeletal muscle, heart, and kidney, and also reduced blood ammonia concentrations. The GAPC combination proved slightly inferior to GA alone in terms of decreasing tissue ammonia levels, but effectively restored normal blood ammonia and serum glucose levels. These findings are in accordance with the literature data. GA and related compounds have been shown to increase cell sensitivity to insulin and decrease hepatic gluconeogenesis, resulting in lower serum glucose and insulin levels [12,14,45]. PC could provide an additional improvement in glucose tolerance by activating PPARα [47,48] and by suppressing SREBP-1c, a key regulator of glycolytic gene expression in the liver [49]. The decrease in blood and tissue ammonia content could be related to the overall improvement in liver function, as, to the best of our knowledge, no direct hypoammonaemic mechanisms have been yet proposed for either GA or PC.

Both GA and GAPC reduced serum MDA levels and erythrocyte neutral carbonyl content, while GA was more effective for lowering erythrocyte basic carbonyl content. Only the GAPC combination, but not GA alone, was capable of restoring normal serum catalase activity. This additive effect could be related to the potentiation of the intrinsic antioxidant activity of PC [50] by the enzyme induction caused by GA via the Nrf2 pathway [13].

Oxidative stress and insulin resistance in NAFLD have also been reported to be associated with increased activity of two novel biomarkers, NADPH oxidase 2 (Nox2) and 8-iso-prostaglandin $F_{2\alpha}$ (8-iso-PGF$_{2\alpha}$) [51,52]. Moreover, the current evidence suggests an important role for gut-microbial endotoxin accumulation in the pathogenesis of chronic liver disease [53]. Therefore, serum Nox2, urinary 8-iso-PGF$_{2\alpha}$, and serum endotoxin levels appear to be highly relevant for further research on NAFLD treatment using GA and/or PC.

GA and, to a lesser extent, GAPC increased liver ApoA1 expression. ApoA1 is the main protein of high-density and very-high-density lipoprotein, and plays a critical role in the efflux of fat molecules by accepting fats from within cells and transporting them elsewhere, including back to low-density lipoprotein particles or to the liver for excretion [54]. Recently, ApoA1 has become recognised as a mediator of hepatic lipid deposition [55], and also an important factor in the pathogenesis of MASLD/MASH [54]. All subtypes of PPAR have been implicated as promoters to increase ApoA1 secretion and expression from the liver [54]. Therefore, PPARγ upregulation by GA could lead to ApoA1 induction, contributing to the observed improvement in liver steatosis. Whether simultaneous PPARα activation by PC could amplify the effects of GA appears to be controversial and requires elucidation.

Increased desmin synthesis and formation of desmin-containing filaments is one of the hallmarks of transdifferentiation of hepatic stellate cells into myofibroblast-like cells during fibrogenesis [56]. Increased Fndc5/irisin signalling-pathway activity could be a sign of some compensatory mechanisms being activated in the skeletal muscle to combat local and systemic inflammation [57]. Our results indicate that both GA and GAPC could,

to some extent, reduce Des and Fndc5 expression, restoring it to normal levels. A similar pattern of expression was observed for collagen IV, an accepted biomarker of advanced liver fibrosis [58].

IL1β and SCD1 expression in the liver was unchanged in the model we used, and unaffected by either of the treatments. Increased IL1β expression has been linked to MASH progression in experimental animals [59], and SCD1 is currently becoming recognised as a prominent regulator of autophagy and autophagy-induced apoptosis [60]. We believe that the absence of notable change in IL1β and/or SCD1 expression in our study might have been caused by the use of a relatively 'mild' MASH model [20]. However, it is worth noting that both GA and PC appear to have no effect on autophagy.

Myostatin expression in the skeletal muscle tends to increase with the progression of muscle atrophy, local fat accumulation, and sarcopenia [61], while myogenin, on the other hand, undergoes downregulation [62]. Consistent with these findings, we observed a slight tendency towards an increase in Mstn and a decrease in Myog transcript levels in skeletal muscle of Control group mice, although no signs of advanced sarcopenia were present during morphological examination.

In the OF, EPM, and LDB tests, general locomotion and novelty exploration were suppressed in Control group mice, which is consistent with both our previous results [31] and the data in the literature [63]. A marked decrease in exploration was also observed in the NOR test. The GAPC combination, but not GA alone, increased peeking-out frequency and the number of chamber transitions in the LDB test, indicating improved exploration. However, it also reduced the latency to the first DC visit and increased its duration, which could be interpreted as anxiety-like behaviour [25], a possibility which requires further investigation.

Clear depression-like behaviour was not characteristic of mice with MASH in our study, as only a slight tendency towards immobility latency reduction was detected in the TS and FS tests. However, GA reduced the frequency of immobility episodes and total immobility time, and GAPC increased immobility latency in the abovementioned tests, and promoted grooming in the SS test. A mild antidepressant activity of GA has been demonstrated in recent animal [64,65], as well as clinical, studies [66]. As neuroinflammation is considered a major target for GA as an antidepressant agent [65], it is possible that PC could augment its effects by enhancing neuronal differentiation under inflammatory stress conditions [67].

Visuospatial memory and learning impairments are a known feature of experimental rodent [68], as well as human, MASH [5]. In our study, we observed a long-term decrease in spatial memory, as shown in the SATM test, but no change in object-recognition memory. Consistent with our previous results [69], this discrepancy could possibly be explained by the stronger dependency of spatial memory rather than recognition memory on functional hippocampal tissue volume [70].

GAPC treatment restored both spatial learning performance in the SATM test and exploration in the NOR test, while GA alone was less effective. Pro-cognitive activity of GA has been demonstrated previously in aging mice [11], as well as those with scopolamine-induced amnesia [71], and with systemic inflammatory conditions [72]. Just as with the antidepressant activity, the main mechanism of GA's pro-cognitive action appears to be related to the suppression of neuroinflammation and prevention of its deleterious effects on neuron structure and function [72,73]. Whether PC could augment this activity via its own anti-inflammatory mode of action remains to be investigated. The reduction in systemic and brain ammonia levels could be of additional benefit to the neurocognitive function, since ammonia is a potent neurotoxin and the major factor for the development of hepatic encephalopathy [74].

Both GA and GAPC treatment regimens increased CMAP peak amplitudes in m. gastrocnemius and m. biceps brachii, which is indicative of their positive effects on the number and volume of functional motor units. This effect could be the result of the amelioration of myosteatosis (see above), local and systemic inflammation, and oxidative

stress, which all contribute negatively to muscle performance [75–77]. In addition, the reduction in blood and tissue ammonia content (most importantly, in the skeletal muscle and the heart), and therefore its toxicity, could prove beneficial for myofibre metabolism and function [78,79].

To summarize the above, the combination of GA and PC demonstrated a synergistic additive mode of action, one which could be interpreted as partial synergism, since the expected effect amplification was only observed in regard to some parameters. The two agents showed moderate synergism in their anti-inflammatory, antioxidant, hypoammon-aemic, hypoglycaemic, and pro-cognitive effects. Combined therapy was effective for preventing and reducing liver steatosis, hepatitis activity, and muscle steatosis, which, along with the observed ApoA1 upregulation, could imply the combination's therapeutic potential for MASLD/MASH as well as for other disorders of lipid metabolism.

Differential effects of GA alone and its combination with PC were seen in regard to higher functions, namely, anxiety- and depression-like behaviour, as well as Apoa1 expression. Neither of the treatments produced a significant effect on the animals' physical performance. 18β-Glycyrrhetinic acid, the major pharmacologically active metabolite of GA, has previously been shown to cross the blood–brain barrier (BBB) in vivo [80], which could imply the presence of its intrinsic neurotropic activity in addition to an overall improvement in the neurological functions due to increased liver protection. Exogenous choline supplementation, which is further incorporated into PC, beneficially impacts neurogenesis and reparation processes directly in the central nervous system in traumatic brain injuries and associated comorbidities [81].

Based on a thorough literature review and our own findings, we propose the following scheme for the pharmacological synergism between GA and PC (Figure 17).
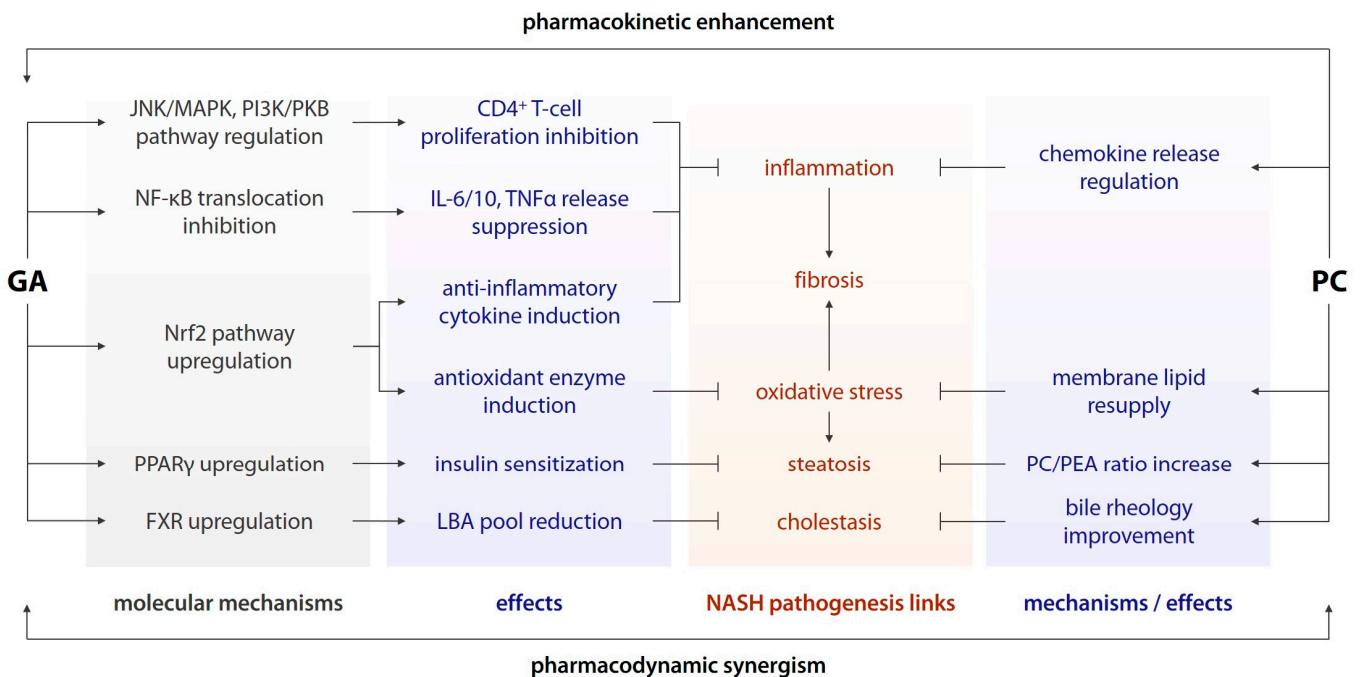

Figure 17. Implications for the pharmacological synergism between glycyrrhizinic acid and phosphatidylcholine. GA, glycyrrhizinic acid; PC, phosphatidylcholine; JNK, c-Jun N-terminal kinase; MAPK, mitogen-activated protein kinase; PI3K, phosphoinositide 3-kinase; PKB; protein kinase B; NF-κB, nuclear factor-κB; Nrf2, nuclear factor erythroid 2-related factor 2; PPARγ, peroxisome proliferator-activated receptor γ; FXR, farnesoid X-receptor; IL, interleukin; TNFα, tumour necrosis factor α; LBA, lipophilic bilce acid; PEA, phosphatidylethanolamine.

References

1. European Association for the Study of the Liver (EASL); European Association for the Study of Diabetes (EASD); European Association for the Study of Obesity (EASO). EASL-EASD-EASO Clinical Practice Guidelines for the management of non-alcoholic fatty liver disease. *J. Hepatol.* **2016**, *64*, 1388–1402. [CrossRef]
2. Monelli, F.; Venturelli, F.; Bonilauri, L.; Manicardi, E.; Manicardi, V.; Giorgi Rossi, P.; Massari, M.; Ligabue, G.; Riva, N.; Schianchi, S.; et al. Systematic review of existing guidelines for NAFLD assessment. *Hepatoma Res.* **2021**, *7*, 25. [CrossRef]
3. Eslam, M.; Sanyal, A.J.; George, J.; International Consensus Panel. MAFLD: A Consensus-Driven Proposed Nomenclature for Metabolic Associated Fatty Liver Disease. *Gastroenterology* **2020**, *158*, 1999–2014.e1. [CrossRef]
4. Lombardi, R.; Fargion, S.; Fracanzani, A.L. Brain Involvement in Non-Alcoholic Fatty Liver Disease (NAFLD): A Systematic Review. *Dig. Liver Dis.* **2019**, *51*, 1214–1222. [CrossRef]
5. Kjærgaard, K.; Mikkelsen, A.C.D.; Wernberg, C.W.; Grønkjær, L.L.; Eriksen, P.L.; Damholdt, M.F.; Mookerjee, R.P.; Vilstrup, H.; Lauridsen, M.M.; Thomsen, K.L. Cognitive Dysfunction in Non-Alcoholic Fatty Liver Disease-Current Knowledge, Mechanisms and Perspectives. *J. Clin. Med.* **2021**, *10*, 673. [CrossRef]
6. Gonzalez, A.; Huerta-Salgado, C.; Orozco-Aguilar, J.; Aguirre, F.; Tacchi, F.; Simon, F.; Cabello-Verrugio, C. Role of Oxidative Stress in Hepatic and Extrahepatic Dysfunctions during Nonalcoholic Fatty Liver Disease (NAFLD). *Oxid. Med. Cell Longev.* **2020**, *2020*, 1617805. [CrossRef] [PubMed]
7. Muzurović, E.; Mikhailidis, D.P.; Mantzoros, C. Non-Alcoholic Fatty Liver Disease, Insulin Resistance, Metabolic Syndrome and Their Association with Vascular Risk. *Metabolism* **2021**, *119*, 154770. [CrossRef] [PubMed]
8. Graebin, C.S. The Pharmacological Activities of Glycyrrhizinic Acid ("Glycyrrhizin") and Glycyrrhetinic Acid. *Sweeteners* **2017**, 245–261. [CrossRef]
9. Kim, S.-W.; Jin, Y.; Shin, J.-H.; Kim, I.-D.; Lee, H.-K.; Park, S.; Han, P.-L.; Lee, J.-K. Glycyrrhizic Acid Affords Robust Neuroprotection in the Postischemic Brain via Anti-Inflammatory Effect by Inhibiting HMGB1 Phosphorylation and Secretion. *Neurobiol. Dis.* **2012**, *46*, 147–156. [CrossRef] [PubMed]
10. Sathyamoorthy, Y.; Kaliappan, K.; Nambi, P.; Radhakrishnan, R. Glycyrrhizic Acid Renders Robust Neuroprotection in Rodent Model of Vascular Dementia by Controlling Oxidative Stress and Curtailing Cytochrome-c Release. *Nutr. Neurosci.* **2020**, *23*, 955–970. [CrossRef] [PubMed]
11. Jiang, R.; Gao, J.; Shen, J.; Zhu, X.; Wang, H.; Feng, S.; Huang, C.; Shen, H.; Liu, H. Glycyrrhizic Acid Improves Cognitive Levels of Aging Mice by Regulating T/B Cell Proliferation. *Front. Aging Neurosci.* **2020**, *12*, 570116. [CrossRef] [PubMed]
12. Li, J.; Cao, H.; Liu, P.; Cheng, G.; Sun, M. Glycyrrhizic Acid in the Treatment of Liver Diseases: Literature Review. *Biomed. Res. Int.* **2014**, *2014*, 872139. [CrossRef]
13. Chen, S.; Zou, L.; Li, L.; Wu, T. The Protective Effect of Glycyrrhetinic Acid on Carbon Tetrachloride-Induced Chronic Liver Fibrosis in Mice via Upregulation of Nrf2. *PLoS ONE* **2013**, *8*, e53662. [CrossRef] [PubMed]
14. Yoke Yin, C.; So Ha, T.; Abdul Kadir, K. Effects of Glycyrrhizic Acid on Peroxisome Proliferator-Activated Receptor Gamma (PPARgamma), Lipoprotein Lipase (LPL), Serum Lipid and HOMA-IR in Rats. *PPAR Res.* **2010**, *2010*, 530265. [CrossRef] [PubMed]

15. Wu, S.-Y.; Cui, S.-C.; Wang, L.; Zhang, Y.-T.; Yan, X.-X.; Lu, H.-L.; Xing, G.-Z.; Ren, J.; Gong, L.-K. 18β-Glycyrrhetinic Acid Protects against Alpha-Naphthylisothiocyanate-Induced Cholestasis through Activation of the Sirt1/FXR Signaling Pathway. *Acta Pharmacol. Sin.* **2018**, *39*, 1865–1873. [CrossRef] [PubMed]

16. Shinu, P.; Gupta, G.L.; Sharma, M.; Khan, S.; Goyal, M.; Nair, A.B.; Kumar, M.; Soliman, W.E.; Rahman, A.; Attimarad, M.; et al. Pharmacological Features of 18β-Glycyrrhetinic Acid: A Pentacyclic Triterpenoid of Therapeutic Potential. *Plants* **2023**, *12*, 1086. [CrossRef] [PubMed]

17. Nicolson, G.L.; Ash, M.E. Lipid Replacement Therapy: A Natural Medicine Approach to Replacing Damaged Lipids in Cellular Membranes and Organelles and Restoring Function. *Biomembranes* **2014**, *1838*, 1657–1679. [CrossRef]

18. Osipova, D.; Kokoreva, K.; Lazebnik, L.; Golovanova, E.; Pavlov, C.; Dukhanin, A.; Orlova, S.; Starostin, K. Regression of Liver Steatosis Following Phosphatidylcholine Administration: A Review of Molecular and Metabolic Pathways Involved. *Front. Pharmacol.* **2022**, *13*, 797923. [CrossRef]

19. Singh, R.P.; Gangadharappa, H.V.; Mruthunjaya, K. Phospholipids: Unique Carriers for Drug Delivery Systems. *J. Drug. Deliv. Sci. Technol.* **2017**, *39*, 166–179. [CrossRef]

20. Tsuchida, T.; Lee, Y.A.; Fujiwara, N.; Ybanez, M.; Allen, B.; Martins, S.; Fiel, M.I.; Goossens, N.; Chou, H.-I.; Hoshida, Y.; et al. A Simple Diet- and Chemical-Induced Murine NASH Model with Rapid Progression of Steatohepatitis, Fibrosis and Liver Cancer. *J. Hepatol.* **2018**, *69*, 385–395. [CrossRef]

21. Nair, A.B.; Jacob, S. A Simple Practice Guide for Dose Conversion between Animals and Human. *J. Basic Clin. Pharm.* **2016**, *7*, 27–31. [CrossRef] [PubMed]

22. Phosphogliv Forte. Registration Certificate. Available online: https://grls.rosminzdrav.ru/Grls_View_v2.aspx?routingGuid=49 b3de04-9280-43ea-a3c6-e88c872a924c (accessed on 6 December 2023).

23. Walsh, R.N.; Cummins, R.A. The Open-Field Test: A Critical Review. *Psychol. Bull.* **1976**, *83*, 482–504. [CrossRef] [PubMed]

24. Walf, A.A.; Frye, C.A. The Use of the Elevated plus Maze as an Assay of Anxiety-Related Behavior in Rodents. *Nat. Protoc.* **2007**, *2*, 322–328. [CrossRef] [PubMed]

25. Bourin, M.; Hascoët, M. The Mouse Light/Dark Box Test. *Eur. J. Pharmacol.* **2003**, *463*, 55–65. [CrossRef] [PubMed]

26. Can, A.; Dao, D.T.; Terrillion, C.E.; Piantadosi, S.C.; Bhat, S.; Gould, T.D. The Tail Suspension Test. *J. Vis. Exp.* **2012**, *59*, e3769. [CrossRef]

27. Can, A.; Dao, D.T.; Arad, M.; Terrillion, C.E.; Piantadosi, S.C.; Gould, T.D. The Mouse Forced Swim Test. *J. Vis. Exp.* **2012**, *59*, e3638. [CrossRef]

28. Isingrini, E.; Camus, V.; Le Guisquet, A.-M.; Pingaud, M.; Devers, S.; Belzung, C. Association between Repeated Unpredictable Chronic Mild Stress (UCMS) Procedures with a High Fat Diet: A Model of Fluoxetine Resistance in Mice. *PLoS ONE* **2010**, *5*, e10404. [CrossRef]

29. Deacon, R.M.J.; Rawlins, J.N.P. T-Maze Alternation in the Rodent. *Nat. Protoc.* **2006**, *1*, 7–12. [CrossRef]

30. Leger, M.; Quiedeville, A.; Bouet, V.; Haelewyn, B.; Boulouard, M.; Schumann-Bard, P.; Freret, T. Object Recognition Test in Mice. *Nat. Protoc.* **2013**, *8*, 2531–2537. [CrossRef]

31. Prikhodko, V.A.; Sysoev, Y.I.; Poveryaeva, M.A.; Bunyat, A.V.; Karev, V.E.; Ivkin, D.Y.; Sukhanov, D.S.; Shustov, E.B.; Okovityi, S.V. Effects of empagliflozin and L-ornithine L-aspartate on behavior, cognitive functions, and physical performance in mice with experimentally induced steatohepatitis. *Bull. RSMU* **2020**, *3*, 49–57. [CrossRef]

32. Pollari, E.; Prior, R.; Robberecht, W.; Van Damme, P.; Van Den Bosch, L. In Vivo Electrophysiological Measurement of Compound Muscle Action Potential from the Forelimbs in Mouse Models of Motor Neuron Degeneration. *J. Vis. Exp.* **2018**, *136*, 57741. [CrossRef]

33. Gutiérrez-de-Juan, V.; López de Davalillo, S.; Fernández-Ramos, D.; Barbier-Torres, L.; Zubiete-Franco, I.; Fernández-Tussy, P.; Simon, J.; Lopitz-Otsoa, F.; de las Heras, J.; Iruzubieta, P.; et al. A Morphological Method for Ammonia Detection in Liver. *PLoS ONE* **2017**, *12*, e0173914. [CrossRef]

34. Botsoglou, N.A.; Fletouris, D.J.; Papageorgiou, G.E.; Vassilopoulos, V.N.; Mantis, A.J.; Trakatellis, A.G. Rapid, Sensitive, and Specific Thiobarbituric Acid Method for Measuring Lipid Peroxidation in Animal Tissue, Food, and Feedstuff Samples. *J. Agricult. Food Chem.* **1994**, *42*, 1931–1937. [CrossRef]

35. Góth, L. A Simple Method for Determination of Serum Catalase Activity and Revision of Reference Range. *Clin. Chim. Acta* **1991**, *196*, 143–151. [CrossRef]

36. Kostiuk, V.A.; Potapovich, A.I.; Kovaleva, Z.V. A simple and sensitive method of determination of superoxide dismutase activity based on the reaction of quercetin oxidation. *Vopr. Med. Khim.* **1990**, *36*, 88–91. (In Russian) [PubMed]

37. Levine, R.L.; Garland, D.; Oliver, C.N.; Amici, A.; Climent, I.; Lenz, A.G.; Ahn, B.W.; Shaltiel, S.; Stadtman, E.R. Determination of Carbonyl Content in Oxidatively Modified Proteins. *Methods Enzymol.* **1990**, *186*, 464–478. [CrossRef]

38. Hervé, M. RVAideMemoire: Testing and Plotting Procedures for Biostatistics. R Package Version 0.9-83. 2023. Available online: https://CRAN.R-project.org/package=RVAideMemoire (accessed on 28 June 2023).

39. Prikhodko, V.A.; Karev, V.E.; Sysoev, Y.I.; Ivkin, D.Y.; Okovityi, S.V. A Simple Algorithm for Semiquantitative Analysis of Scored Histology Data in the R Environment, on the Example of Murine Non-Alcoholic Steatohepatitis Pharmacotherapy. *Livers* **2022**, *2*, 412–424. [CrossRef]

40. Brown, G.T.; Kleiner, D.E. Histopathology of Nonalcoholic Fatty Liver Disease and Nonalcoholic Steatohepatitis. *Metabolism* **2016**, *65*, 1080–1086. [CrossRef]

41. Feng, T.-T.; Yang, X.-Y.; Hao, S.-S.; Sun, F.-F.; Huang, Y.; Lin, Q.-S.; Pan, W. TLR-2-Mediated Metabolic Reprogramming Participates in Polyene Phosphatidylcholine-Mediated Inhibition of M1 Macrophage Polarization. *Immunol. Res.* **2020**, *68*, 28–38. [CrossRef]

42. Lu, Y.; Feng, T.; Zhao, J.; Jiang, P.; Xu, D.; Zhou, M.; Dai, M.; Wu, J.; Sun, F.; Yang, X.; et al. Polyene Phosphatidylcholine Ameliorates High Fat Diet-Induced Non-Alcoholic Fatty Liver Disease via Remodeling Metabolism and Inflammation. *Front. Physiol.* **2022**, *13*, 810143. [CrossRef]

43. Treede, I.; Braun, A.; Sparla, R.; Kühnel, M.; Giese, T.; Turner, J.R.; Anes, E.; Kulaksiz, H.; Füllekrug, J.; Stremmel, W.; et al. Anti-Inflammatory Effects of Phosphatidylcholine. *J. Biol. Chem.* **2007**, *282*, 27155–27164. [CrossRef]

44. Chen, M.; Pan, H.; Dai, Y.; Zhang, J.; Tong, Y.; Huang, Y.; Wang, M.; Huang, H. Phosphatidylcholine regulates NF-κB activation in attenuation of LPS-induced inflammation: Evidence from in vitro study. *Anim. Cells Syst.* **2017**, *22*, 7–14. [CrossRef]

45. Eu, C.H.A.; Lim, W.Y.A.; Ton, S.H.; bin Abdul Kadir, K. Glycyrrhizic Acid Improved Lipoprotein Lipase Expression, Insulin Sensitivity, Serum Lipid and Lipid Deposition in High-Fat Diet-Induced Obese Rats. *Lipids Health Dis.* **2010**, *9*, 81. [CrossRef]

46. Sun, X.; Duan, X.; Wang, C.; Liu, Z.; Sun, P.; Huo, X.; Ma, X.; Sun, H.; Liu, K.; Meng, Q. Protective Effects of Glycyrrhizic Acid against Non-Alcoholic Fatty Liver Disease in Mice. *Eur. J. Pharmacol.* **2017**, *806*, 75–82. [CrossRef]

47. Ye, J.M.; Doyle, P.J.; Iglesias, M.A.; Watson, D.G.; Cooney, G.J.; Kraegen, E.W. Peroxisome Proliferator-Activated Receptor (PPAR)-Alpha Activation Lowers Muscle Lipids and Improves Insulin Sensitivity in High Fat-Fed Rats: Comparison with PPAR-Gamma Activation. *Diabetes* **2001**, *50*, 411–417. [CrossRef]

48. Peeters, A.; Baes, M. Role of PPARα in Hepatic Carbohydrate Metabolism. *PPAR Res.* **2010**, *2010*, 572405. [CrossRef] [PubMed]

49. Dentin, R.; Girard, J.; Postic, C. Carbohydrate Responsive Element Binding Protein (ChREBP) and Sterol Regulatory Element Binding Protein-1c (SREBP-1c): Two Key Regulators of Glucose Metabolism and Lipid Synthesis in Liver. *Biochimie* **2005**, *87*, 81–86. [CrossRef]

50. Saito, H.; Ishihara, K. Antioxidant activity and active sites of phospholipids as antioxidants. *J. Am. Oil Chem. Soc.* **1997**, *74*, 1531–1536. [CrossRef]

51. Del Ben, M.; Polimeni, L.; Carnevale, R.; Bartimoccia, S.; Nocella, C.; Baratta, F.; Loffredo, L.; Pignatelli, P.; Violi, F.; Angelico, F. NOX2-Generated Oxidative Stress Is Associated with Severity of Ultrasound Liver Steatosis in Patients with Non-Alcoholic Fatty Liver Disease. *BMC Gastroenterol.* **2014**, *14*, 81. [CrossRef]

52. Yang, Z.; Yang, J.; Cai, J.; Zhang, X.-J.; Zhang, P.; She, Z.-G.; Li, H. The Transition of Cardiovascular Disease Risks from NAFLD to MAFLD. *Rev. Cardiovasc. Med.* **2023**, *24*, 157. [CrossRef]

53. Kessoku, T.; Kobayashi, T.; Imajo, K.; Tanaka, K.; Yamamoto, A.; Takahashi, K.; Kasai, Y.; Ozaki, A.; Iwaki, M.; Nogami, A.; et al. Endotoxins and Non-Alcoholic Fatty Liver Disease. *Front. Endocrinol.* **2021**, *12*, 770986. [CrossRef] [PubMed]

54. Chen, C.; Li, H.; Song, J.; Zhang, C.; Li, M.; Mao, Y.; Liu, A.; Du, J. Role of Apolipoprotein A1 in PPAR Signaling Pathway for Nonalcoholic Fatty Liver Disease. *PPAR Res.* **2022**, *2022*, 4709300. [CrossRef] [PubMed]

55. Karavia, E.A.; Papachristou, D.J.; Liopeta, K.; Triantaphyllidou, I.-E.; Dimitrakopoulos, O.; Kypreos, K.E. Apolipoprotein A-I Modulates Processes Associated with Diet-Induced Nonalcoholic Fatty Liver Disease in Mice. *Mol. Med.* **2012**, *18*, 901–912. [CrossRef] [PubMed]

56. Geerts, A.; Eliasson, C.; Niki, T.; Wielant, A.; Vaeyens, F.; Pekny, M. Formation of Normal Desmin Intermediate Filaments in Mouse Hepatic Stellate Cells Requires Vimentin. *Hepatology* **2001**, *33*, 177–188. [CrossRef] [PubMed]

57. Rabiee, F.; Lachinani, L.; Ghaedi, S.; Nasr-Esfahani, M.H.; Megraw, T.L.; Ghaedi, K. New Insights into the Cellular Activities of Fndc5/Irisin and Its Signaling Pathways. *Cell Biosci.* **2020**, *10*, 51. [CrossRef] [PubMed]

58. Stefano, J.T.; Guedes, L.V.; de Souza, A.A.A.; Vanni, D.S.; Alves, V.A.F.; Carrilho, F.J.; Largura, A.; Arrese, M.; Oliveira, C.P. Usefulness of Collagen Type IV in the Detection of Significant Liver Fibrosis in Nonalcoholic Fatty Liver Disease. *Ann. Hepatol.* **2021**, *20*, 100253. [CrossRef] [PubMed]

59. Mridha, A.R.; Wree, A.; Robertson, A.A.B.; Yeh, M.M.; Johnson, C.D.; Van Rooyen, D.M.; Haczeyni, F.; Teoh, N.C.-H.; Savard, C.; Ioannou, G.N.; et al. NLRP3 Inflammasome Blockade Reduces Liver Inflammation and Fibrosis in Experimental NASH in Mice. *J. Hepatol.* **2017**, *66*, 1037–1046. [CrossRef] [PubMed]

60. Huang, G.-M.; Jiang, Q.-H.; Cai, C.; Qu, M.; Shen, W. SCD1 Negatively Regulates Autophagy-Induced Cell Death in Human Hepatocellular Carcinoma through Inactivation of the AMPK Signaling Pathway. *Cancer Lett.* **2015**, *358*, 180–190. [CrossRef]

61. Ryan, A.S.; Li, G. Skeletal Muscle Myostatin Gene Expression and Sarcopenia in Overweight and Obese Middle-Aged and Older Adults. *JCSM Clin. Rep.* **2021**, *6*, 137–142. [CrossRef]

62. Langley, B.; Thomas, M.; Bishop, A.; Sharma, M.; Gilmour, S.; Kambadur, R. Myostatin Inhibits Myoblast Differentiation by Down-Regulating MyoD Expression. *J. Biol. Chem.* **2002**, *277*, 49831–49840. [CrossRef]

63. Veniaminova, E.; Cespuglio, R.; Markova, N.; Mortimer, N.; Cheung, C.W.; Steinbusch, H.W.; Lesch, K.-P.; Strekalova, T. Behavioral features of mice fed with a cholesterol-enriched diet: Deficient novelty exploration and unaltered aggressive behavior. *Transl. Neurosci. Clin.* **2016**, *2*, 87–95. [CrossRef]

64. Wang, B.; Lian, Y.-J.; Dong, X.; Peng, W.; Liu, L.-L.; Su, W.-J.; Gong, H.; Zhang, T.; Jiang, C.-L.; Li, J.-S.; et al. Glycyrrhizic Acid Ameliorates the Kynurenine Pathway in Association with Its Antidepressant Effect. *Behav. Brain Res.* **2018**, *353*, 250–257. [CrossRef] [PubMed]

65. Gupta, G.L.; Sharma, L.; Sharma, M. 18β-Glycyrrhetinic Acid Ameliorates Neuroinflammation Linked Depressive Behavior Instigated by Chronic Unpredictable Mild Stress via Triggering BDNF/TrkB Signaling Pathway in Rats. *Neurochem. Res.* **2023**, *48*, 551–569. [CrossRef] [PubMed]

66. Cao, Z.-Y.; Liu, Y.-Z.; Li, J.-M.; Ruan, Y.-M.; Yan, W.-J.; Zhong, S.-Y.; Zhang, T.; Liu, L.-L.; Wu, R.; Wang, B.; et al. Glycyrrhizic Acid as an Adjunctive Treatment for Depression through Anti-Inflammation: A Randomized Placebo-Controlled Clinical Trial. *J. Affect. Disord.* **2020**, *265*, 247–254. [CrossRef] [PubMed]

67. Magaquian, D.; Delgado Ocaña, S.; Perez, C.; Banchio, C. Phosphatidylcholine Restores Neuronal Plasticity of Neural Stem Cells under Inflammatory Stress. *Sci. Rep.* **2021**, *11*, 22891. [CrossRef] [PubMed]

68. Leone, P.; Mincheva, G.; Balzano, T.; Malaguarnera, M.; Felipo, V.; Llansola, M. Rifaximin Improves Spatial Learning and Memory Impairment in Rats with Liver Damage-Associated Neuroinflammation. *Biomedicines* **2022**, *10*, 1263. [CrossRef] [PubMed]

69. Prikhodko, V.A. Effects of ornithine aspartate and empagliflozin on memory deficit symptoms in experimental steatohepatitis. *J. Biomed.* **2022**, *18*, 128–132. [CrossRef]

70. Broadbent, N.J.; Squire, L.R.; Clark, R.E. Spatial Memory, Recognition Memory, and the Hippocampus. *Proc. Natl. Acad. Sci. USA* **2004**, *101*, 14515–14520. [CrossRef] [PubMed]

71. Ban, J.Y.; Park, H.K.; Kim, S.K. Effect of Glycyrrhizic Acid on Scopolamine-Induced Cognitive Impairment in Mice. *Int. Neurourol. J.* **2020**, *24*, S48–S55. [CrossRef]

72. Song, J.-H.; Lee, J.-W.; Shim, B.; Lee, C.-Y.; Choi, S.; Kang, C.; Sohn, N.-W.; Shin, J.-W. Glycyrrhizin Alleviates Neuroinflammation and Memory Deficit Induced by Systemic Lipopolysaccharide Treatment in Mice. *Molecules* **2013**, *18*, 15788–15803. [CrossRef]

73. Liu, W.; Huang, S.; Li, Y.; Zhang, K.; Zheng, X. Suppressive Effect of Glycyrrhizic Acid against Lipopolysaccharide-Induced Neuroinflammation and Cognitive Impairment in C57 Mice via Toll-like Receptor 4 Signaling Pathway. *Food Nutr. Res.* **2019**, *63*, 1516. [CrossRef]

74. Jayakumar, A.R.; Norenberg, M.D. Hyperammonemia in Hepatic Encephalopathy. *J. Clin. Exp. Hepatol.* **2018**, *8*, 272–280. [CrossRef]

75. Correa-de-Araujo, R.; Addison, O.; Miljkovic, I.; Goodpaster, B.H.; Bergman, B.C.; Clark, R.V.; Elena, J.W.; Esser, K.A.; Ferrucci, L.; Harris-Love, M.O.; et al. Myosteatosis in the Context of Skeletal Muscle Function Deficit: An Interdisciplinary Workshop at the National Institute on Aging. *Front. Physiol.* **2020**, *11*, 963. [CrossRef] [PubMed]

76. Serra, A.J.; Pinto, J.R.; Prokić, M.D.; Arsa, G.; Vasconsuelo, A. Oxidative Stress in Muscle Diseases: Current and Future Therapy 2019. *Oxid. Med. Cell. Longev.* **2020**, *2020*, 6030417. [CrossRef]

77. Tuttle, C.S.L.; Thang, L.A.N.; Maier, A.B. Markers of Inflammation and Their Association with Muscle Strength and Mass: A Systematic Review and Meta-Analysis. *Ageing Res. Rev.* **2020**, *64*, 101185. [CrossRef] [PubMed]

78. Chen, H.-W.; Dunn, M.A. Muscle at Risk: The Multiple Impacts of Ammonia on Sarcopenia and Frailty in Cirrhosis. *Clin. Transl. Gastroenterol.* **2016**, *7*, e170. [CrossRef] [PubMed]

79. Di Cola, S.; Nardelli, S.; Ridola, L.; Gioia, S.; Riggio, O.; Merli, M. Ammonia and the Muscle: An Emerging Point of View on Hepatic Encephalopathy. *J. Clin. Med.* **2022**, *11*, 611. [CrossRef] [PubMed]

80. Mizoguchi, K.; Kanno, H.; Ikarashi, Y.; Kase, Y. Specific Binding and Characteristics of 18β-Glycyrrhetinic Acid in Rat Brain. *PLoS ONE* **2014**, *9*, e95760. [CrossRef]

81. Javaid, S.; Farooq, T.; Rehman, Z.; Afzal, A.; Ashraf, W.; Rasool, M.F.; Alqahtani, F.; Alsanea, S.; Alasmari, F.; Alanazi, M.M.; et al. Dynamics of Choline-Containing Phospholipids in Traumatic Brain Injury and Associated Comorbidities. *Int. J. Mol. Sci.* **2021**, *22*, 11313. [CrossRef]